Energy Conversion and Management 80 (2014) 110–116

Contents lists available at ScienceDirect

Energy Conversion and Management

journal homepage: www.elsevier.com/locate/enconman

A novel self-powered wireless temperature sensor based on thermoelectric generators

Yongming Shi [a], Yao Wang [a], Yuan Deng [a,*], Hongli Gao [a], Zhen Lin [a], Wei Zhu [a], Huihong Ye [b]

[a] School of Materials Science & Engineering, Beihang University, Beijing 100191, PR China
[b] Clean-Aviation New Material Technology CO. LTD., Nanjing 210038, PR China

ARTICLE INFO

Article history:
Received 11 October 2013
Accepted 10 January 2014
Available online 10 February 2014

Keywords:
Self-powered sensor
Temperature sensor
Thermoelectric generator
Fire detection

ABSTRACT

A novel self-powered wireless temperature sensor has been designed and presented for solving the power supply problem of temperature sensors. This sensor can autonomously measure temperature under positive temperature fluctuation situations. The self-powered characteristic, realized by using four thermoelectric generators, enables the sensor to operate without any batteries or other power sources. In order to obtain these features, attentions are not only focused on the method to combine signal sensing and power generating together, but also on the method to improve measurement accuracy. Experimental results confirm that this novel sensor has excellent measurement accuracy. The measured performance is consistent with the calculated characteristics. For typical application, this self-powered temperature sensor can detect fire before it develops to flashover state. And the maximum detection distance grows with the growth of burning rate. All the results indicate this innovative sensor is a promising self-powered device which can be used to measure temperature value in positive temperature fluctuation situations.

1. Introduction

As the demand for sustainable and maintenance-free sensor networks is soaring, the energy supply problem of sensors is attracting more and more attentions [1,2]. However, commercially available temperature sensors commonly require batteries as its power source although replacing batteries is a tedious and costly job [3]. Therefore, it is of high priority to develop a self-powered temperature sensor which can operate without any batteries.

Generally speaking, there are two methods to realize a sensor operating without batteries. One is the energy conversion system which can convert other kinds of energy into electrical energy [4,5], such as pressures [6], vibrations [7], winds [8], electromagnetic waves [9], ultraviolet rays [10], and heats [11,12]. The other is passive sensors which are mainly based on the surface acoustic wave (SAW) technique [13–15].

Unfortunately, each of these techniques has its own limitations and challenges. The energy conversion system needs to add an extra energy conversion module to the existing sensor system, which is against the mobility and miniaturization requirements. The SAW sensor sends a low frequency signal with low power which makes its practical propagation distance restricted to several meters [16]. And this distance is not comparable with the transmitting distance of wireless temperature sensors which are powered by batteries.

In recent years, there are some cases of thermoelectric (TE) modules used for harnessing energy for wireless sensors [17,18]. The TE modules in those studies are used as power module rather than sense module. And there has been no report that TE modules are used as both the power module and sense module in a self-powered wireless temperature sensor. The object of this study is to present the design consideration and result analysis of a novel self-powered temperature sensor based on TE modules. The TE modules, adopted in this study, are used as not only the power module but also the sense module. The final device can simultaneously perform temperature measuring and self-powering supplying functions under the positive temperature fluctuation.

2. Principle and implementation

2.1. Principle of TE generators

The principle of TE generators (TEG) can be explained by Fig. 1. An electromotive current will be generated when two dissimilar conductors are connected at two points and a temperature difference is applied on these points (Fig. 1a). This phenomenon is called Seebeck effect, and the voltage is called thermal voltage. The two connected dissimilar conductors constitute a pair of TE legs. If

* Corresponding author. Tel./fax: +86 10 82313482.
E-mail address: dengyuan@buaa.edu.cn (Y. Deng).

http://dx.doi.org/10.1016/j.enconman.2014.01.010
0196-8904/

Nomenclature

U_{op}	open-circuit voltage (V)	S	effective area of the hot side (m^2)
U_o	output voltage (V)	A	cross sectional area of a TE leg (m^2)
V'	negative electrode potential (V)	l	length of a TE leg (m)
I	minimum current for starting (A)	R	distance (m)
R_L	load resistance (Ω)	R_{dmax}	maximum detection distance (m)
R_m	resistance of a TE module (Ω)	$\dot{m}$	burning rate (g/s)
P_{max}	calculated maximum output power (W)	h_c	calorific value (J/g)
T	temperature need to be measured (K)	α	Seebeck coefficient of a TE device (V/K)
ΔT	temperature difference (K)	κ	thermal conductance (W/K)
T_0	cold-side temperature (K)	λ	thermal conductivity of a TE leg (W/m K)
T_1	temperature of hot side (K)	α_r	absorptance of heat absorption coating
Q_{min}	minimum heat power for starting (W)	ε	emissivity of heat absorption coating
q_{min}	minimum thermal flux for starting (W/m^2)	χ_r	efficiency of thermal radiation
Q	thermal radiation power (W)		
P	effective thermal radiation power (W)		
E_b	black-body radiation (W/m^2)		

many pairs of TE legs connect in series, as shown in Fig. 1b, more voltage will be generated when the temperature difference is applied on the hot and cold contacts of the device. The output thermoelectric voltage under open-circuit condition can be expressed as:

$$U_{op} = \alpha \Delta T, \tag{1a}$$

where U_{op} is the open-circuit voltage of TEG, α is the total Seebeck coefficient of a TE device. The parameter ΔT is the temperature difference across the hot and cold connects of the device.

In reality, there must be a load connected to the TEG, and the actual output thermoelectric voltage U_o can be expressed as following equation [19]:

$$U_o = U_{op} \frac{R_L}{R_L + R_m}, \tag{1b}$$

The parameter R_L is the load resistance. The parameter R_m is the resistance of a TE module. When R_L is much higher than R_m, Eq. (1b) can be simplified to Eq. (1c).

$$U_o \approx U_{op} = \alpha \Delta T \tag{1c}$$

As shown in Eq. (1c), the output voltage can be approximated as the open-circuit voltage when the load resistance is much times higher than the internal resistance of TEG. In practical applications, if the parameter R_L is high but difficult to measure, the thermoelectric voltage U_{op} can be obtained by measuring U_o. And the temperature difference ΔT can also be obtained by measuring U_o.

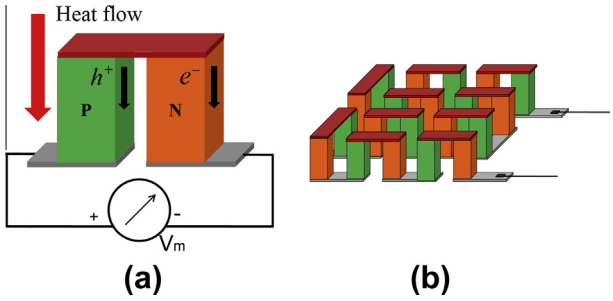

Fig. 1. The principle of Seebeck effect (a) and the principle of thermoelectric module (b).

2.2. Principle of self-powered wireless temperature sensor

The simple principle of the self-powered wireless temperature sensor (SPWTS) can be explained by Fig. 2.

A TEG and a temperature compensation component (TCC) compose a self-powered temperature probe (SPTP). The function of the TEG is to measure the temperature difference between its two sides and to convert the temperature gradient into electric power. Meanwhile the function of the TCC is to provide a temperature reference which is just like the cold end compensation for thermocouple thermometers. To ensure the accuracy, the TCC is a digital temperature sensor as usual. When the TEG is exposed to a temperature difference, it will generate a thermal voltage which is mathematically related to the temperature difference. This thermal voltage, an analog signal, is transmitted to the microprocessor by an A/D converter module. And based on Eq. (1c), the thermal voltage can be approximated as the open-circuit voltage, because the input resistance of an A/D converter is usually much times higher than the internal resistance of TEG. This thermal voltage is also supplied to other modules as power supply through a power management module. And the power management module also provides a reference voltage for the A/D converter. The cold-side temperature of the TEG is detected by the TCC. Then the cold-side temperature value is directly transmitted to the microprocessor in digital signals. To calculate the temperature, these two signals are processed by the microprocessor according to the following equation:

$$T = \frac{U_o}{\alpha} + T_0, \tag{2}$$

where T is the temperature value which needs to be measured, and U_o is the output voltage which is generated by the TEG. The parameter α is the total Seebeck coefficient of the TEG, and T_0 is the cold-side temperature. As the cold-side temperature T_0 is relatively low, the maximum measurement temperature mainly depends on the TE module whose maximum operating temperature is usually at 200 °C or higher [20,21]. However, if only using a digital sensor to measure the temperature, the maximum measurement temperature of this device will be decreased. The operating temperature of digital temperature sensors is equal to that of standard IC technology, which is below 150 °C [22]. Therefore, based on the temperature compensation principle, the maximum measurement temperature of this device will be higher than the situation that only a digital sensor is used to measure the temperature.

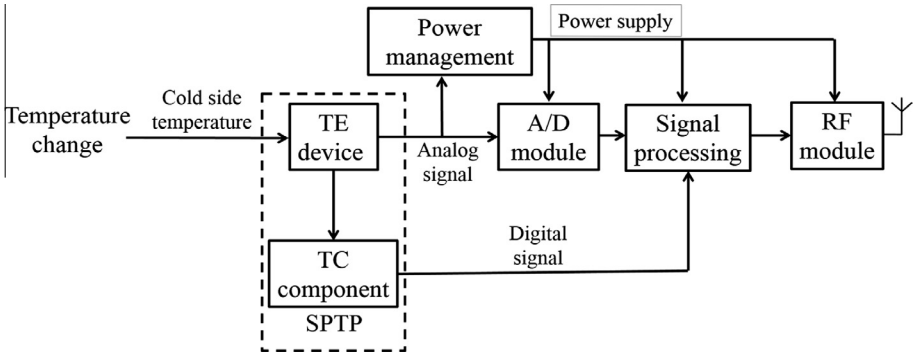

Fig. 2. Block diagram of the SPWTS.

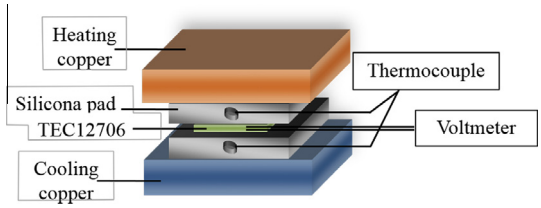

Fig. 3. The sandwiched structure used to measure the Seebeck coefficient and power generation performance.

2.3. Parameter determination

To confirm Eq. (2), the Seebeck coefficient α of the TEG was achieved by measurement through a sandwiched structure as displayed in Fig. 3. The sandwiched structure (from top to bottom) is copper/thermally conductive pad/thermocouple/TEG/thermocouple/thermally conductive pad/copper. To apply a temperature difference on the two sides of the TEG, only one copper plate was heated by resistive heater and the other was kept cool by natural-air cooling at room temperature. Two thermocouples were used to measure the temperature difference between the two sides of the TEG. The open-circuit voltage was measured by a voltmeter under open-circuit condition when the TEG was working. And the internal resistance (2.18 Ω) was measured by a LCR meter (Agilent U1731C) when the TEG was not working. As shown in Fig. 3, the surface temperature of TE device is obtained through measured the temperature of the silicona pad. Consequently, there exist an approximation between the temperature values of the TE surface and the silicona pad, which is the limitation of this measurement approach.

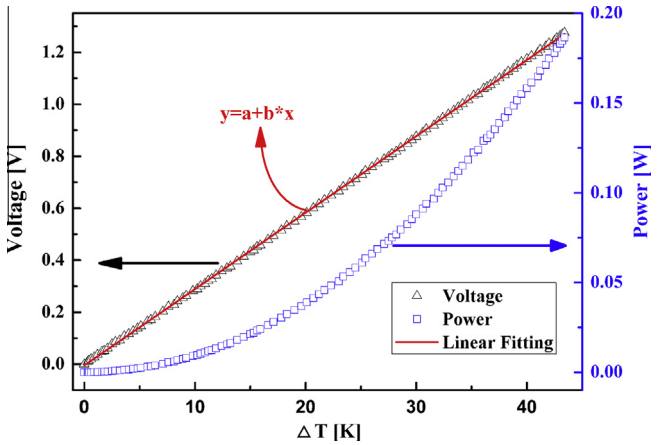

Fig. 4. The power generation performance of a signal TEG.

Fig. 4 depicts the output voltage and the calculated maximum output power (P_{max}) at different ΔT. The calculated maximum output power can be obtained when the TEG is hypothetically connected to a matched load ($R_L = R_m$). The calculation equation can be expressed by Eq. (3).

$$P_{max} = \frac{U_{op}^2}{4R_m} \tag{3}$$

Although the Seebeck coefficient of a TEG changes with temperature, it can be regarded as a constant within a limited temperature range. Therefore, by processing voltage values through linear fitting, the Seebeck coefficient can be obtained according to Eq. (1a).

The fitting equation is

$$U_O = V' + \alpha\Delta T. \tag{4}$$

Here, U_O is equal to the output voltage of the TEG. The parameter V' is the intercept which is equal to the negative electrode potential of the TEG, and α is the slope which is equal to the Seebeck coefficient. The parameter ΔT is the temperature difference applied on the TEG. The results of the linear fitting are displayed in Table 1. The output voltage of the TEG can be rewritten as Eq. (5) based on the liner fitting result.

$$U_O = V' + 0.029(V/K)\Delta T \tag{5}$$

The intercept value V' will be zero while the negative electrode potential is zero. Therefore, the Eq. (2) can be confirmed as:

$$T = \frac{U_o}{0.029(\mathrm{V/K})} + T_0. \tag{6}$$

2.4. Implementation of SPWTS

The structures of the SPWTS can be described through Fig. 5a. The SPTP is composed of a TEG, a TCC and an aluminum heat sink. The TEG employed in this application is TEC12706 which contains 127 pairs of TE legs, and the TCC is a digital temperature sensor (DS18B20, produced by Dallas Semiconductor) whose highest working temperature is 398 K. The dimension ($L \times W \times H$) of the heat sink is 40 mm, 40 mm and 11 mm, and it has 126 fins. To ensure the accuracy of TCC and maximize the output power of TEG, the TCC and the heat sink are glued closely to the cold side of the TEG by thermally conductive silica gel (thermal conductivity >2 W/m K). The power supply of the SPWTS is generated by four SPTPs. These four SPTPs connect electrically in series but thermally

Table 1
The results of liner fitting.

a (V)	b (V/K)	N	SE	R
$-0.00445 \pm 7.25 \times 10^{-4}$	$0.02939 \pm 2.86 \times 10^{-5}$	102	0.9999	1.54×10^{-3}

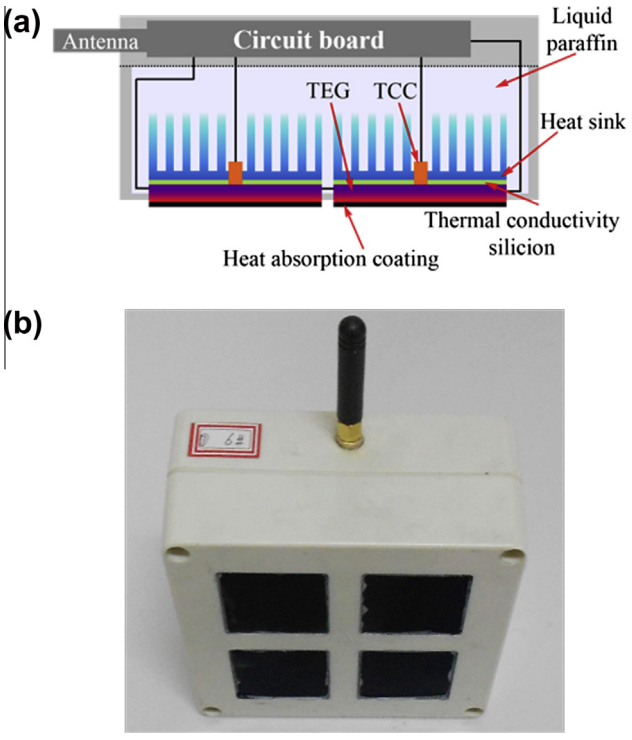

Fig. 5. The schema (a) and the photograph (b) of the SPWTS.

in parallel. The SPTPs are arranged on the same surfaces of the encapsulation which is manufactured by engineering plastics (PC/ABS). The final measured temperature value is equal to the average temperature of these four SPTPs. To increase the heat absorption, heat absorption coating (Blue Core, produced by Jin-Xiang New Energy) is used onto the hot side of the TEGs. The coating is sputtered on an aluminum substrate which make can make the hot-side temperature uniform. To stabilize the cold-side temperature of the SPTP for maintaining a durable temperature difference, solid paraffin (melting temperature ranging between 331 K and 333 K) is filled in the unoccupied spaces of the encapsulation. As solid paraffin is a kind of phase-change materials which usually serves as heat storage materials [23], it can maintain the cold-side temperature of the TEG at a low level. The heat transferred to the cold side will be absorbed by the solid paraffin when the hot side is heated. In addition, the paraffin can still absorb heat even if it is heated into liquid phase, because the liquid paraffin has a relatively high specific heat capacity (about 2.8×10^3 J kg^{-1} K^{-1}). Therefore, heats can be still absorbed after the paraffin is heated from solid phase into liquid phase. The temperature difference between the two sides of the TEG will be increased through using solid paraffin. Consequently the output voltage will be enhanced.

The circuit section is mainly based on an ultra-low power wireless chip (nRF24LE1, produced by NORDIC SEMICONDUCTOR) which contains a fourteen-channel A/D converter, a fast microcontroller, a RF transceiver, and the corresponding power management module. During A/D conversion, the input resistance of the whole circuit is above 500 Ω which is much times higher than the internal resistance of TEG. Therefore, the output voltage of TEG can be approximated as the open-circuit voltage based on Eqs. (1b) and (1c). Fig. 5b shows the photograph of a prototype of the SPWTS.

3. Results and discussion

For a self-powered temperature sensor, measurement accuracy, start condition, and its performance under the application environment are three criterions which are worth noting.

3.1. Accuracy of the SPTP without paraffin

The measurement accuracy of the SPTP is the most important parameter that directly affects the accuracy of this temperature sensor. To investigate the accuracy of the SPTP, both the SPTP and a calibrated thermocouple were placed onto the copper which was heated by a heater (WY-99, produced by Tianjin Ke-Qi Instrument and Equipment Co.). The temperature of the copper was simultaneously measured by the SPTP and the thermocouple for contrast purpose. The measured value of the thermocouple is treated as the accurate temperature. Fig. 6 shows the measurement error of the SPTP. Within the temperature range of 293 K to 405 K, the maximum absolute error of the SPTP is 1.6 K and the mean absolute error (MAE) is 0.55 K as displayed in Fig. 6. This result indicates that the temperature values of the copper, measured by these two methods, are in good agreement within an acceptable difference. The error is mainly caused by the cold-side temperature nonuniformity of the TEG while some areas of cold side are warmed up quickly and some areas slowly. However the TCC can only measure the temperature of a small area. Therefore, the TCC can't measure the cold-side temperature accurately.

3.2. Accuracy of the SPTP with paraffin

Due to the introduction of the solid paraffin, the measurement error of the SPTP is decreased. The solid paraffin can absorb more heat, because it has a higher specific heat capacity than air (approximately 1×10^3 J kg^{-1} K^{-1}). When the cold-side temperature nonuniformity occurs, the solid paraffin can absorb heat from those hotter areas, and make the cold-side temperature more uniform. Therefore, the TCC can measure the cold-side temperature of the TEG more accurately. To prove this contribution of the solid paraffin, the SPWTS was placed into a thermal shock chamber (UHS1200, produced by Angelantoni Climatic Systems) whose heating rate can be controlled. A thermocouple was placed onto the heat-absorbing surface of the sensor. The chamber was heated at the heating rate of about 30 K/min at first. After the SPWTS switched on, the heating rate was slowed down to 5 K/min to prevent the temperature from going extremely high. Fig. 7b shows the measurement accuracy of the SPTP with paraffin after the SPWTS started to operate. The result indicates that the maximum absolute error is 0.5 K and the MAE is 0.37 K during the operating period. For the purposes of comparison, the accuracy of the SPTP without paraffin during the same temperature range is shown in Fig. 7b. This result indicates that the measurement error of the SPTP can

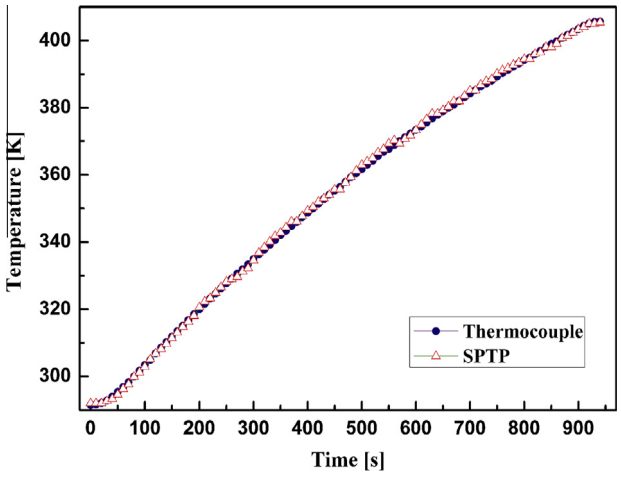

Fig. 6. The measurement error of a single SPTP without paraffin.

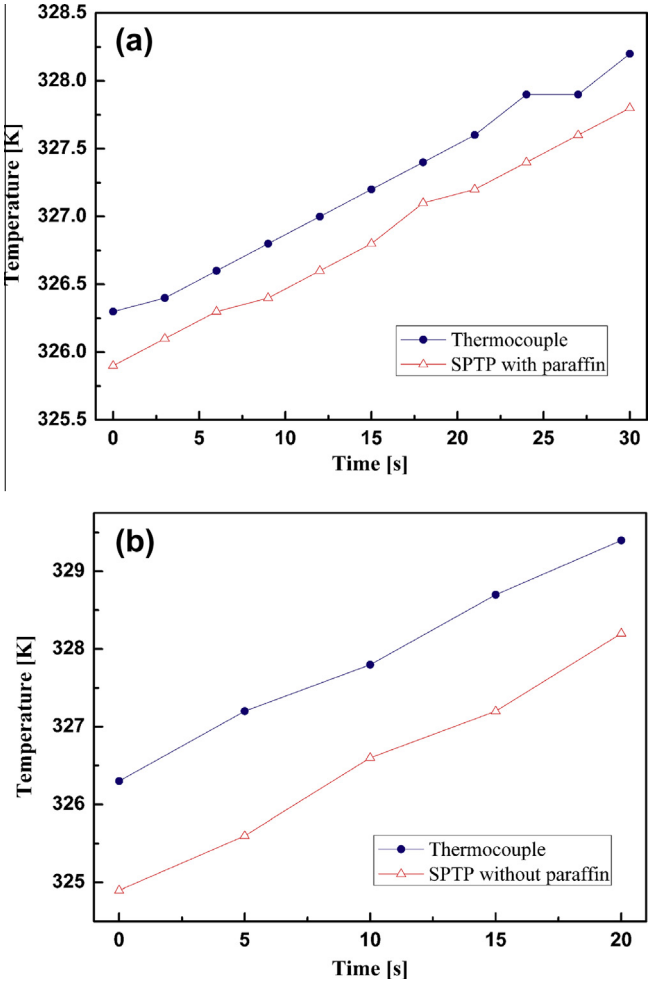

Fig. 7. The measurement error of the SPTP with paraffin (a) vs. without paraffin (b) during operating period.

be decreased through introducing the high heat capacity materials such as solid paraffin.

3.3. Minimum heat flux for starting

As the SPWTS needs a sufficient temperature difference to switch on, there should be a heat source to provide a sufficient thermal flux. In order to investigate the minimum thermal flux that the SPWTS needs to operate, a heating lamp (275 W, produced by Opple Illumination) was used as the heat source to heat the SPWTS. The sensor was placed at different distances (from $d = 10$ cm to $d = 20$ cm) away from the heating lamp. Fig. 8 shows the measured curves of the output voltage with respect to the time. The dashed horizontal line is the minimum voltage (2.6 V) for the steady operation of the electric circuit. Table 2 shows the relationships between detection distance and response time, which indicates that the response time grows with the detection distance. The responding received thermal flux is also shown in Table 2. The SPWTS will not respond if the distance is beyond 20 cm. The reason of this phenomenon is attributed to the lack of sufficient heat flux. When the SPWTS is too far away from the heating lamp, the lamp can't provide sufficient heat flux to make the SPWTS start. When the distance is 20 cm, the corresponding heat flux is estimated by a heat flux sensor (HS-30B, produced by Captec) to be 1.28×10^4 W/m^2. To verify the reliability of this value, theoretical calculation is deduced as following.

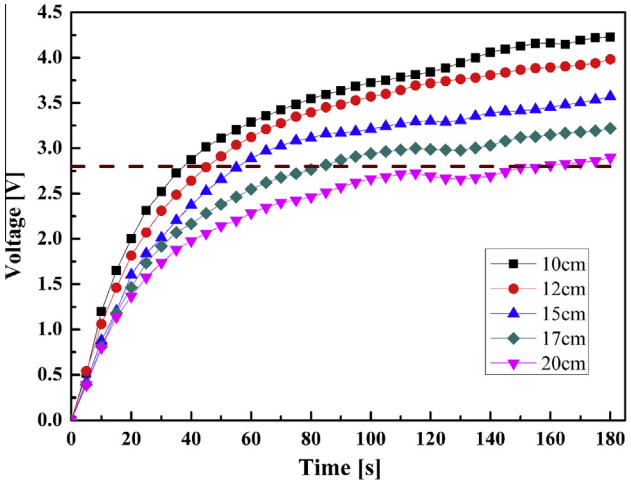

Fig. 8. The power generation performance of SPTP.

Table 2
The responding time and received thermal flux of self-powered temperature sensor.

Distance (cm)	Response time (s)	Thermal flux ($\times 10^4$ W/m^2)
10	37	4.21
12	46	3.43
15	56	2.36
17	85	1.72
20	160	1.28

The required minimum thermal flux can be expressed as:

$$q_{min} = Q_{min}/S, \tag{7}$$

where Q_{min} is the required minimum heat power which is absorbed by the hot side of the TEG, and S is the effective area of the hot side. The parameter Q_{min} can be written as Eq. (8) [24].

$$Q_{min} = \alpha T_1 I - \frac{1}{2} I^2 R_m + \kappa \Delta T \tag{8}$$

Here, α is the Seebeck coefficient, and T_1 is the temperature of hot side at which the sensor starts to operate. The parameter I is the sensor required minimum current, and R_m is the resistance of the TEG. And κ is the total thermal conductance of TE materials which can be expressed as Eq. (9).

$$\kappa = 127 \frac{A_N}{l_N} \lambda_N + 127 \frac{A_P}{l_p} \lambda_P \tag{9}$$

In Eq. (9), the parameter 127 is the number of thermocouples. The parameters A and l are the area and length of TE material, and λ is the thermal conductivity of the thermoelectric material used in the TEG. The subscripts represent the N-type or P-type thermoelectric materials. In this study, A and l are 1.96×10^{-6} m^2 and 2.4×10^{-3} m respectively. The thermal conductivity of both N-type and P-type materials are 1.4 W/m K as common. Consequently, according to Eq. (9), the total thermal conductance is 2.9×10^{-1} W/K.

Substituting Eq. (8) into Eq. (7), then Eq. (10) can be expressed as:

$$q_{min} = \frac{\alpha T_1 I - \frac{1}{2} I^2 R_m + \kappa \Delta T}{S}. \tag{10}$$

The parameters R_m and α are defined as 2.18 Ω and 0.029 V/K by testing. Meanwhile, by means of experiment, the system required minimum ΔT is 23 K, and the corresponding T_1 is 326 K. The whole current of the circuit ranges from 6 mA (A/D conversion period) to

17 mA (wireless communication period). Herein, parameter I is defined as 100 mA to ensure startup. As Eq. (8) is the module which only take the thermal conductance of the TE materials into consideration, the corresponding area should be the effective area rather than the whole surface area of the TE module. The effective area is 4.98×10^{-4} m^2 which only covers TE materials. Consequently, the minimum q that the system required can be calculated as 1.53×10^4 W/m^2. Comparing with 1.28×10^4 W/m^2 which is obtained by experiment, the difference between the results of experiment and theoretical calculation is merely 0.28×10^4 W/m^2. And this difference is acceptable. In addition, on the basis of minimum thermal flux that the SPWTS needs to operate, the performance of the SPWTS under the typical application, such as fire detection, can be obtained through simulation.

3.4. Simulation for typical application

Since this SPWTS is sensitive to the temperature variation, it can be used as a sensor to detect temperature anomalies such as fire disaster. The burning combustibles can generate a sufficient thermal flux to make this SPWTS switched on. Therefore, the performance of the SPWTS under a real fire disaster can be achieved by simulation, since it is difficult to obtain by experiments. The real fire disaster is simulated through using the steady-state fire model. The minimum heat flux made the SPWTS switched on can be expressed as:

$$q_{min} = \frac{P\alpha_r}{4\pi R^2} - \varepsilon E_b = \frac{\chi_r Q \alpha_r}{4\pi R^2} - \varepsilon E_b. \tag{11a}$$

Herein, the parameter q_{min} is the minimum required thermal flux which is generated by combustibles. P is the effective thermal radiation power. The parameter R is the distance between the SPWTS and the heat source. The parameters α_r and ε are the absorptance and emissivity of the heat absorption coating respectively. E_b is the black-body radiation at the same temperature of the heat absorption coating. Q is the total thermal radiation power of the combustibles. The parameter χ_r is the efficiency of the thermal radiation which is between 0.3 and 0.4 for steady state burning [25]. And it is defined as 1/3 in this paper.

$$q_{min} \approx \frac{P}{4\pi R^2} \approx \frac{\chi_r Q}{4\pi R^2} \tag{11b}$$

Because the heat absorption coating used in this study has high absorbance (higher than 0.95) and low emissivity (lower than 0.05), the radiation from TEG to the surrounding besides the heat source can be neglected. Therefore, Eq. (11a) can be approximated as Eq. (11b). Then Eq. (11b) can be rewritten as:

$$Q = 12\pi R^2 q_{min}. \tag{12}$$

For a certain combustible, the thermal radiation power Q is assumed as a constant under the steady-state fire situation. The relationship between Q and the burning rate $\dot{m}$ can be described as Eq. (12). The parameter h_c is the calorific value of combustibles.

$$Q = \dot{m} h_c. \tag{13}$$

Substituting Eq. (13) into Eq. (12), then Eq. (14) can be obtained after rearranging.

$$R_{dmax} = \sqrt{\frac{\dot{m} h_c}{12\pi q_{min}}}. \tag{14}$$

In Eq. (14), R_{dmax} is the maximum detection distance for fire detection application. This equation can be used to describe the relationship between the burning rate $\dot{m}$ and the maximum detection distance R_{dmax}. If h_c and q_{min} are definite, the curve of $\dot{m}$ with respect to R_{dmax} can be drawn up as Fig. 9. The maximum detection distance R_{dmax} grows with the growth of burning rate $\dot{m}$. And the maximum detection distance varies with different combustibles. If the maximum detection distance is designed as 1 m, it can respond to burning rates from 11 g/s (for gasoline) to 39 g/s (for wood).

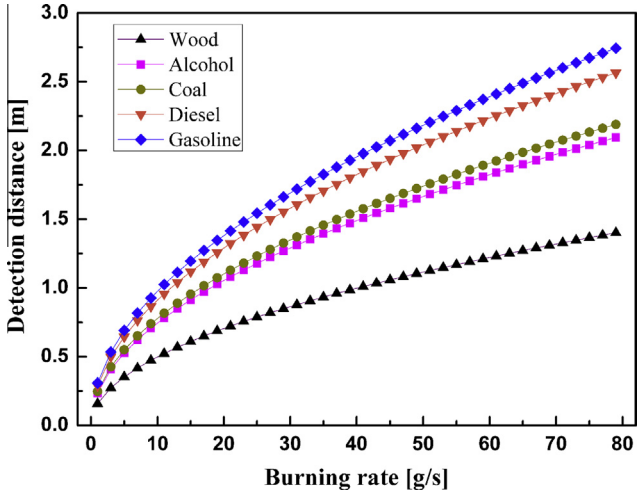

Fig. 9. The maximum detection distance of SPWTS under different burning rates.

For fire detection, flashover (the heat flux value reach over 20 kW/m^2 [26]) is a critical stage. The fire is difficult to be put out when it evolves to the flashover stage. For this self-powered sensor, the measured and theoretical minimum starting heat flux values are 12.8 kW/m^2 and 15.3 kW/m^2 respectively. Therefore, this self-powered sensor can start to operate before the fire develops to flashover state.

4. Conclusions

Herein, a self-powered wireless temperature sensor, working without any batteries, has been actually fabricated and tested. This sensor can autonomously perform measuring temperature and transmitting wireless data, and it is powered by its temperature probe which is based on commercial thermoelectric modules to convert heat energy into electrical energy. Without introducing solid paraffin which serves as a temperature stabilizer, the maximum absolute error of the temperature probe is 1.6 K and the MAE is 0.55 K. After introducing solid paraffin, the performance of the temperature probe is improved and the accuracy is further promoted. The corresponding maximum absolute error is 0.5 K and the MAE is 0.37 K when the sensor is operating with solid paraffin. The theoretical calculation indicates this self-powered sensor needs 1.53×10^4 W/m^2 of thermal flux to switch on, which accords with the experiment result (1.28×10^4 W/m^2) within an acceptable difference. For typical application, this self-powered temperature sensor can detect fire before it develops to flashover state. And the maximum detection distance grows with the growth of burning rate. All the results indicate this innovative sensor is a promising self-powered device which can be used to measure temperature value in temperature fluctuation situations. More importantly, this sensor is promising to solve the power supplying problem of mobile sensors.

Acknowledgements

The work was supported by the State Key Development Program for Basic Research of China (Grant No. 2012CB933200), National Natural Science Foundation of China (No. 51172008 and

51002006), Research Fund for Doctor Station Sponsored by the Ministry of Education of China (20111102110035) and the Fundamental Research Funds for the Central Universities.

References

[1] Paradise JA, Stamer T. Energy scavenging for mobile and wireless electronics. Pervasive Comput. 2005;4:18–27.
[2] Hu Y, Zhang Y, Xu C, Lin L, Snyder RL, Wang ZL. Self-powered system with wireless data transmission. Nano Lett. 2011;6:2572–7.
[3] Zhu D, Beeby SP, Tudor MJ, et al. A credit card sized self powered smart sensor node. Sensors Actuat. A: Phys. 2011;169:317–25.
[4] Sudevalayam S, Kulkarni P. Energy harvesting sensor nodes: survey and implications. IEEE Commun. Surveys Tutorials 2011;13:443–61.
[5] Hudak NS, Amatucci GG. Small-scale energy harvesting through thermoelectric, vibration, and radiofrequency power conversion. J. Appl. Phys. 2008;103. 101301–101301.
[6] Howells CA. Piezoelectric energy harvesting. Energy Convers. Manage. 2009;50:1847–50.
[7] Lv HY, Tian XY, Wang MY, Li D. Vibration energy harvesting using a phononic crystal with point defect states. Appl. Phys. Lett. 2013;102. 034103–034103.
[8] Sardini E, Serpelloni M. Self-powered wireless sensor for air temperature and velocity measurements with energy harvesting capability. IEEE Trans. Instrum. Meas. 2011;60:1838–44.
[9] Chen JD, Chen D, Yuan T, Chen X. A multi-frequency sandwich type electromagnetic vibration energy harvester. Appl. Phys. Lett. 2012;100. 213509–213509.
[10] Bitnar B, Durisch W, Holzner R. Thermophotovoltaics on the move to applications. Appl. Energy 2013;105:430–8.
[11] Fan P, Zheng ZH, Cai ZK, et al. The high performance of a thin film thermoelectric generator with heat flow running parallel to film surface. Appl. Phys. Lett. 2013;102. 033904–033904.
[12] Sue CY, Tsai NC. Human powered MEMS-based energy harvest devices. Appl. Energy 2012;93:390–403.
[13] Binder A, Fachberger R. Wireless SAW temperature sensor system for high-speed high-voltage motors. IEEE Sens. J. 2011;11:966–70.
[14] Binder A, Bruckner G, Schobernig N, Schmitt D. Wireless SAW pressure and temperature sensor with unique identification based on $LiNbO_3$. IEEE Sens. J. 2013;13:1801–5.
[15] Wang SQ, Jiro H, Satoshi U. A wireless surface acoustic wave temperature sensor using langasite as substrate material for high-temperature applications. Jpn. J. Appl. Phys. 2003;42. 6124–6124.
[16] Kozlovski NY, Malocha DC, Weeks AR. A 915 MHz SAW sensor correlator system. IEEE Sens. J. 2012;11:3426–32.
[17] leonov V, Torfs T, Fiorini P, Hoof CV. Thermoelectric converters of human warmth for self-powered wireless sensor nodes. IEEE Sens. J. 2007;7:650–7.
[18] Dalola S, Ferrari V, Guizzetti M, Marioli D, Sardini E, Serpelloni M, et al. Autonomous sensor system with power harvesting for telemetric temperature measurements of pipes. IEEE Trans. Instrum. Meas. 2009;58:1471–8.
[19] Rowe DM, Gao M. Evaluation of thermoelectric modules for power generation. J. Power Sources 1998;73:193–8.
[20] Hadjistassou Constantinos, Kyriakides Elias, Georgiou Julius. Designing high efficiency segmented thermoelectric generators. Energy Convers. Manage. 2013;66:165–72.
[21] Lesage FJ, Pelletier R, Fournier L, et al. Optimal electrical load for peak power of a thermoelectric module with a solar electric application. Energy Convers. Manage. 2013;74:51–9.
[22] Bakker Anton. CMOS smart temperature sensors-an overview. Sensors 2002;2:1423–7.
[23] Farid Mohammed M, Khudhair Amar M, Razack Siddique Ali K, Al-Hallaj Said. A review on phase change energy storage: materials and applications. Energy Convers. Manage. 2004;45:1597–615.
[24] Bonin R, Boero D, Chiaberge M, Tonoli A. Design and characterization of small thermoelectric generators for environmental monitoring devices. Energy Convers. Manage. 2013;73:340–9.
[25] Koseki Hiroshi, Mulholland GW. The effect of diameter on the burning of crude oil pool fire. Fire Technol. 1991;2:54–65.
[26] Peacock RD, Reneke PA, Bukowski RW, Babrauskas V. Defining flashover for fire hazard calculations. Fire Safety J. 1999;32:331–45.